Original scientific paper

# A FINITE ELEMENT MODEL OF *IN VIVO* MOUSE TIBIAL COMPRESSION LOADING: INFLUENCE OF BOUNDARY CONDITIONS

*UDC (531.2+519.6):617.3*

# Hajar Razi[1,2], Annette I. Birkhold[1,2], Manfred Zehn[3], Georg N. Duda[1,2], Bettina M. Willie[1], Sara Checa[1]

[1]Julius Wolff Institut, Charité-Universitätsmedizin Berlin, Germany
[2]Berlin-Brandenburg School for Regenerative Therapies, Berlin, Germany
[3]Technische Universität Berlin, Germany

**Abstract**. *Though bone is known to adapt to its mechanical challenges, the relationship between the local mechanical stimuli and the adaptive tissue response seems so far unclear. A major challenge appears to be a proper characterization of the local mechanical stimuli of the bones (e.g. strains). The finite element modeling is a powerful tool to characterize these mechanical stimuli not only on the bone surface but across the tissue. However, generating a predictive finite element model of biological tissue strains (e.g., physiological-like loading) encounters aspects that are inevitably unclear or vague and thus might significantly influence the predicted findings. We aimed at investigating the influence of variations in bone alignment, joint contact surfaces and displacement constraints on the predicted strains in an in vivo mouse tibial compression experiment. We found that the general strain state within the mouse tibia under compressive loading was not affected by these uncertain factors. However, strain magnitudes at various tibial regions were highly influenced by specific modeling assumptions. The displacement constraints to control the joint contact sites appeared to be the most influential factor on the predicted strains in the mouse tibia. Strains could vary up to 150% by modifying the displacement constraints. To a lesser degree, bone misalignment (from 0 to 20°) also resulted in a change of strain (+300 με = 40%). The definition of joint contact surfaces could lead to up to 6% variation. Our findings demonstrate the relevance of the specific boundary conditions in the in vivo mouse tibia loading experiment for the prediction of local mechanical strain values using finite element modeling.*

**Key Words**: *Finite Element Model, Mouse Tibial Loading, Bone Adaptation, Bone Mechanics*

## 1. INTRODUCTION

The local mechanical strains play a key role in regulating bone mass and architecture. It is known that changes in the mechanical strains "perceived" at a local position within the bone can result in the deposition or resorption of bone matrix at that location and that this depends, to a large extent, on the strain magnitude [1]. *In vivo* animal loading experiments have been extensively used to investigate the bone adaptation response to controlled mechanical loading [1-8]. Among them, the *in vivo* mouse tibial compression model has been widely used [2, 4, 5, 7, 8]. In this model, the tibia of the mouse is placed between a concave cup and a platen for the application of a controlled compressive load [3]. Finite element techniques are then used to predict the mechanical strains induced in different regions within the bone [3, 8-10]. Although these computer models ideally attempt to replicate the experimental set-up, the *in vivo* experiment includes a certain degree of uncertainty regarding some modeling parameters, e.g. the alignment of the bone within the loading machine or the degrees of freedom at the joint surfaces.

A recent finite element study has shown that in order to predict the location of the neutral axis in the mouse tibial loading model, the loading conditions should include both the compressive load being applied during the experiment plus an extra lateral force, which is not included in the experimental protocol [10]. This indicates that the mouse tibia in the loading machine is probably not completely aligned. Previous radiographic analyses of the mouse tibia mounted in the loading machine by our group have also confirmed this [3]. In addition, Yang and co-workers have shown *in situ* by removing the soft tissue from the mouse hindlimb that the mouse tibia exhibits a tilt angle in the loading machine [9]. Despite these observations, the effect of limb alignment on the predicted strains remains to be investigated.

Other uncertain parameters in finite element modeling of the mouse tibial compression model relate to the boundary conditions, both in terms of point of application and degrees of freedom. Experimental measurement of the contact surfaces at the knee and the ankle through which the load is being transferred is a challenge *in vivo*. Finite element studies of the *in vivo* mice tibia loading model have assumed different contact surfaces [9-12]. Patel and co-workers used micro-computed tomography (μCT) to define boundary conditions at the knee and ankle joints of the mouse tibia [10]. They fixed all degrees of freedom in all points within one 2D μCT image located at the ankle joint. Similarly, the load was uniformly distributed between all points at the most proximal 2D μCT image (representing the knee joint) [10]. Yang et al., 2014, used two ellipses to approximate the contact surfaces at the knee, while restraining movement in all points on the articular surface of the distal tibia [9]. To what degree the predicted mechanical strains are influenced by the joint contact areas remains unknown. In addition to the contact surfaces, it remains unknown how much the bone can move in the transverse plane perpendicular to the loading axis. The concave cup and platen are designed to hold the tibia in place; however, small movements could be present. Yang and co-workers investigated the effect of proximal tibial displacement constraints on the predicted strains [9]. They showed that this parameter introduces the largest index in their sensitivity analysis [9]. The influence of this parameter on the strain state within mouse tibia is still unclear.

Accurate prediction of strains using finite element modeling relies not only on the geometrical and material properties, but also on correct definition of loading and boundary conditions. In this study, we aimed at investigating the influence of bone alignment and

boundary conditions, both in terms of point of application and degrees of freedom, on the mechanical strains predicted using a FE model of the *in vivo* mouse tibial compression loading experiment. Variations in the load direction (bone alignment) and boundary conditions have been investigated separately by isolating one factor at a time (assuming that these parameters are independent).

## 2. MATERIALS AND METHOD

### 2.1. Study design

This study presents finite element models which have been created to replicate an in vivo strain gauging experiment of the left tibia of an elderly mouse (78 week old female C57Bl/6J) as described elsewhere (Fig. 1A-B) [7]. Briefly, uni-axial strain gauges (one per tibia) were mounted on the anterio-medial surface of the tibia mid-shaft of live animals (Fig. 1C).
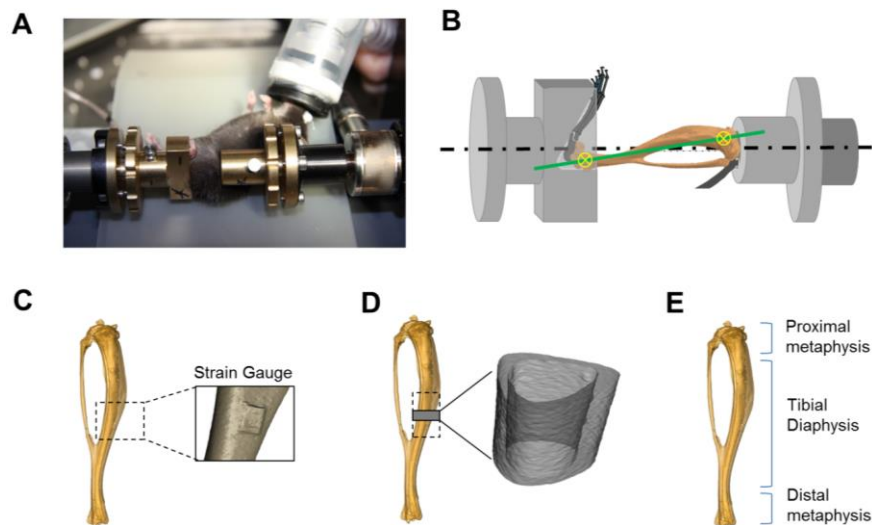


**Fig. 1** (A) Experimental set-up and (B) schematic demonstration of mouse tibia in the loading machine (C) Micro-computed tomography image of the mouse tibia demonstrating the position of the strain gauge position in the scan (D) Cortical mid-shaft region of interest at the tibial mid-diaphysis and (E) tibial diaphyseal, proximal and distal metaphyseal regions.

While the mice remained anesthetized, dynamic compressive loads were applied between the flexed knee and the ankle using a custom-designed *in vivo* loading device (Testbench ElectroForce LM1, Bose, Framingham, USA). Load and strain were recorded simultaneously. A range of dynamic compressive loads (peak loads ranging from -2 to -12N) were applied to identify the applied load that engendered approximately +1400 με *in vivo* at the strain gauge position in mouse tibia. All animal experiments were carried

out according to the policies and procedures approved by the local legal research animal welfare representative (LAGeSo Berlin, G0333/09).

## 2.2. Finite element modeling

### 2.2.1. Geometry and discretization

One left tibia from a mouse that underwent the strain gauging experiment was used to create FE models. To acquire accurate bone morphology, *ex vivo* micro-computed tomography (μCT) was performed on the tibia. μCT was performed with an isotropic voxel resolution of 9.9 μm (Skyscan 1172, Kontich, Belgium; 100 kVp, 100 μA, 360°, using 0.3° rotation steps, 3 frames averaging). Bone geometry was segmented by excluding background and soft tissue voxels from the bone region by applying a global threshold of 0.105 mm$^{-1}$ (linear attenuation coefficient). The threshold value was determined based on the grey value distribution of the whole bone [13, 14]. Following the segmentation, bone surfaces (both cortical and cancellous regions) were defined using a triangular approximation algorithm coupled with best isotropic vertex placement [15] to achieve high triangulation quality. The enclosed bone surfaces were filled with volumetric tetrahedral elements (C3D4 tetrahedrons) resulting in adaptive multi-resolution grids using the ZIBamira software (Zuse Institute, Berlin, Germany). The mechanical interaction between the tibia and the fibula at the tibiofibular joint (proximal) was set considering the amount of mineralized tissue connecting them.

The influence of mesh density on the predicted strains was investigated using eight models with different number of elements. A range of feasible mesh densities; i.e. minimum density aimed at geometrical fidelity ($0.7{\times}10^6$ elements) and maximum density aimed at feasible computational cost ($2.2{\times}10^6$ elements), introduced small changes in the strains predicted at the cortical mid-diaphysis and strain gauge site (2% and 7%, respectively). Thereafter, FE models were performed using approximately $1.5{\times}10^6$ elements in the mouse tibia. Linear elastic FE analysis was performed in Abaqus 6.12.2 (Dassault Systèmes Simulia, RI, USA) to simulate the in vivo tibial loading experiment. To investigate the differences in the induced mechanical strains when varying model parameters, an identical external load (-11 N) was applied to all FEMs. Load was applied through a contact surface selected on the knee side. Displacement constraints were applied at ankle side to the talus-tibialis contact pressure surface. In order to compare the influence of boundary condition variations on the strain state within the bone tissue, bone was assumed isotropic and homogeneous. A linear elastic isotropic Young's modulus (E) of 20 GPa and a Poisson's ratio (ν) of 0.3 was assigned to all regions of the bone.

### 2.2.2. Joint contact surfaces

The joint contact pressure sites at the knee and ankle joints were modified by changing the surface at which boundary conditions were assigned (Fig. 2). In addition, two single points at knee and ankle joints were selected to assign boundary conditions. In these models, the axial compression load was inserted with 0° tilt angle with respect to the tibia longitudinal axis (the description of this axis can be found below; Fig. 3) and surface nodes at ankle side were fixed in all degrees of freedom while surface nodes at the knee side were fixed in translation at perpendicular directions to the load (constraint 1).

### 2.2.3. Distal and proximal displacement constraints

In addition, the displacement constraints at the boundaries were modified in three modes:

- *Constraint* 1: Surface nodes at ankle side were fixed in all degrees of freedom, surface nodes at the knee side (where load was inserted) were fixed in translation at perpendicular directions to the load.
- *Constraint* 2: Surface nodes at ankle side were fixed in all translational degrees of freedom and free for rotational moments, surface nodes at the knee side were fixed in translation at perpendicular directions to load.
- *Constraint* 3: Surface nodes at ankle side were fixed in all degrees of freedom, no displacement constraint was applied at surface nodes at the knee side.

In these models, the axial compression load was inserted with 0° tilt angle with respect to the tibia longitudinal axis (Fig. 3) and knee/ankle contact surfaces were set as shown in A2B2, Fig. 2.
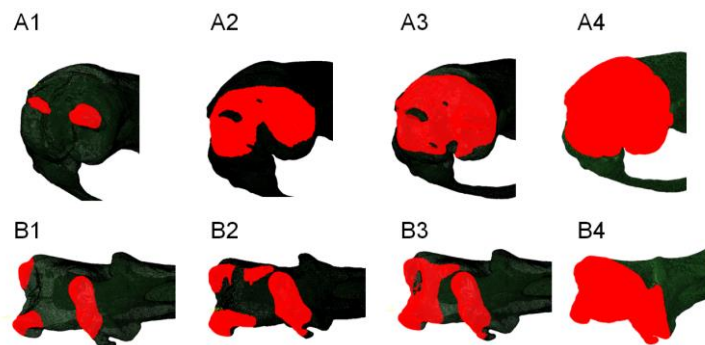


**Fig. 2** Contact pressure sites (highlighted in red) at knee (A1 to A4) and ankle (B1 to B4) joints selected for assigning load and displacement constraints in FEM.

### 2.2.4. Bone Alignment

In order to modify the load direction (bone alignment with respect to the loading machine), a longitudinal axis was assigned to the tibia. The proximal-distal (P-D) axis of the bone was defined as the axis passing through the mid-points between the medial and lateral knee tuberosities and the medial and lateral malleouli. Load direction was then modified by rotating the P-D axis around the perpendicular axis passing through the lateral and medial knee tuberosities (M-L axis) from 0° to 20° (Fig. 3). This a feasible range within which the mouse tibia is visually accommodated by the knee cup and ankle platen. To perform the comparison between different load directions, surface nodes at the ankle side were fixed in all degrees of freedom and surface nodes at the knee side were fixed in translation at perpendicular directions to the load (constraint 1). Joint contact pressures were assigned according to A2B2 (Fig. 2).
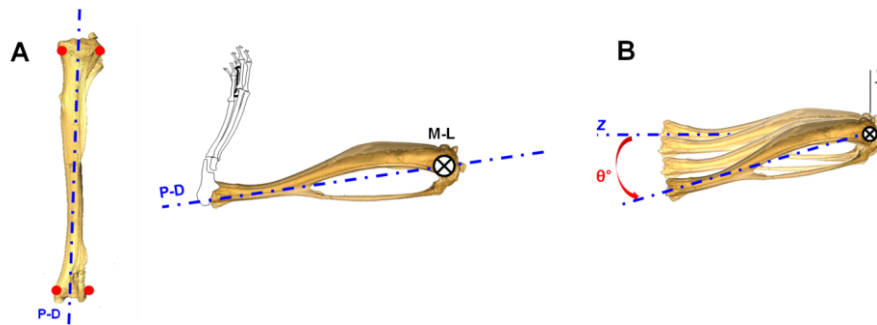
**Fig. 3**    (A) Assignment of the bone longitudinal axis in order to have comparable load
        trajectory across the models of the in vivo experimental set-up. P-D represents
        the proximal-distal axis and M-L the medio-lateral axis (shown by the cross).
        (B) Variations in the bone alignment in the in vivo experimental set-up resulting
        in modified load trajectories in the FE models of the mouse tibia.

### 2.2.5. Data analysis

Alterations in the induced strains as influenced by the boundary conditions were
investigated by comparing the strains in two regions of interest: 1) at the strain gauge
position (Fig. 1C) and 2) at the cortical mid-diaphysis (5% of bone length) in the FE models
(Fig. 1D). Strain components for the elements at the position of the strain gauge (seen in the
*ex vivo* µCT scan of bones) were calculated in the local coordinates of the strain gauge so
that $\varepsilon_{xx}$ is the strain component in the longitudinal strain gauge direction. Average and
standard deviation for all elements at the strain gauge location are reported. In addition,
average and ranges of minimum (compressive) and maximum (tensile) principal strains at
the cortical mid-shaft region are reported for different models.

## 3. RESULTS

### 3.1. Joint contact surfaces

Variation in the joint contact surfaces (Fig. 2) resulted in a maximum of 6% and 10%
difference in the average compressive and tensile principal strains induced at the tibia
mid-diaphysis (Table 1). This difference was observed between applying the boundary
conditions to the entire surface at both knee and ankle joints (A4B4) and to the single
points at joints (Fig. 4). This variation was also reflected at the longitudinal strains
predicted at the strain gauge position (6% variation in longitudinal strains between
models). In addition, up to 70% variation was calculated in the longitudinal strain at the
gauge site compared to *in vivo* measurements (in A4B4). Changes in the joint contact
surfaces led to variations in the distribution of strains (Fig. 5). Specifically higher strains
were observed at proximal and distal tibia regions when applying the boundary conditions
to single nodes compared to larger contact surfaces (Fig. 5). However, at the distal
diaphyseal region higher strains were predicted when implementing the boundary
conditions at the entire knee and ankle surfaces (Fig. 5).

**Table 1** Mean±SD of principal strains induced at the mid-diaphysis

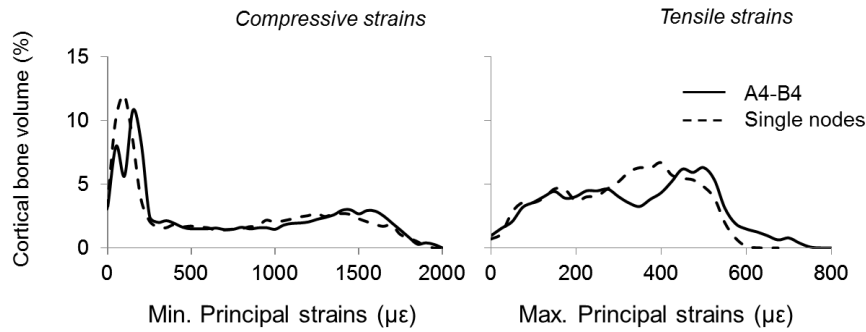| Principal strains | Single nodes | A1B1 | A2B2 | A3B3 | A4B4 |
|---|---|---|---|---|---|
| Tensile | 350±170 | 329±147 | 322±145 | 321±145 | 316±144 |
| Compressive | 760±598 | 728±588 | 720±581 | 718±579 | 711±574 |



**Fig. 4** Distribution of minimum (left) and maximum (right) principal strains at the cortical mid-diaphysis of mouse tibia while implementing the boundary conditions at single nodes in ankle and knee surfaces (dashed line) and in A4B4 (filled line)
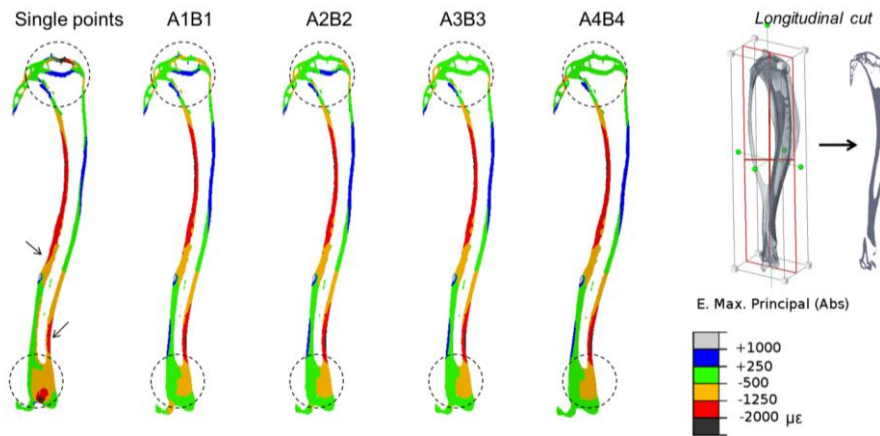


**Fig. 5** Absolute maximum principal strains induced within the mouse tibia while implementing the boundary conditions at single points and four different contact surface conditions at ankle (proximally) and knee (distally) side (A1B1 to A4B4). Plots show longitudinal cut through the tibia. Circles and arrows point to regions with large differences between models

### 3.2. Distal and proximal displacement constraints

Modifying the displacement constraints resulted in large differences in the induced strains at the cortical mid-diaphysis of the tibia (Fig. 6). The largest differences in maximum and minimum principal strains induced at the cortical midshaft occurred between displacement

*constraints* 2 and 3 (20% and 10%, respectively) (Fig. 6). In addition, restraining the foot and ankle and leaving the knee free resulted in higher compressive and tensile principal strains at the anterior and posterior side of the distal tibia (respectively) compared to conditions where the knee was partially restrained of movement (*constraints* 1 and 2) (Fig. 7). The influence of the boundary conditions was more evident in the strain predicted at the strain gauge site. Longitudinal strains increased by 150% and 120 % between displacement *constraints* 3 and 2, and between displacement *constraints* 1 and 2, respectively. Compared to the *in vivo* measurements (+1400 µε), predicted strains at the gauge site were from 28% (*constraints* 3) to 70% (*constraints* 1) lower.
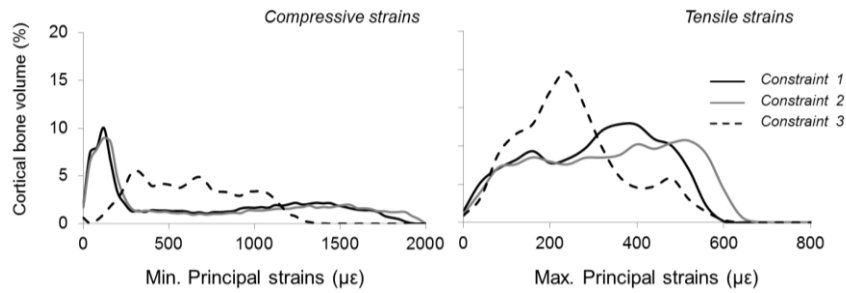


**Fig. 6** Distribution of minimum (A) and maximum (B) principal strains at the cortical mid-diaphysis of mouse tibia while implementing constraint states 1-3 in ankle and knee surfaces
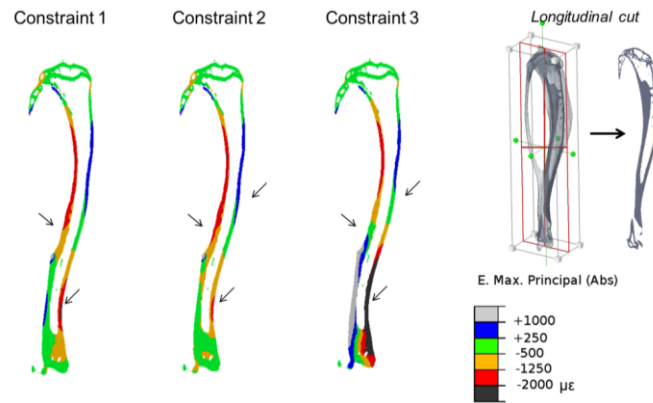


**Fig. 7** Absolute maximum principal strains induced within the mouse tibia while implementing different boundary conditions at A2B2 contact surfaces. Plots show longitudinal cut through the tibia. Arrows point to regions with large differences between models

### 3.3. Bone alignment

Increasing the angle between the bone axis and the load direction resulted in a shift towards higher strain values at the cortical mid-shaft of the mouse tibia (Fig. 8A). The effect of bone misalignment was also evident in the predicted strain at the strain gauge position. By changing the misalignment angle from 0 to 20°, FEM predicted a +300 µε

increase in longitudinal strains at the strain gauge position (Fig. 8B). Compared to the *in vivo* measurements, strains at the gauge site were 40% to 60% lower. The general strain state within the mouse tibia was not largely affected by introducing the misalignment (Fig. 9). However, anterior and posterior proximal diaphyseal regions exhibited high tensile and compressive strain (respectively) by increasing the alignment angles. By increasing the bone misalignment both compression and tension sites (anterior and posterior diaphysis, respectively) were under larger strain magnitudes than the aligned model.
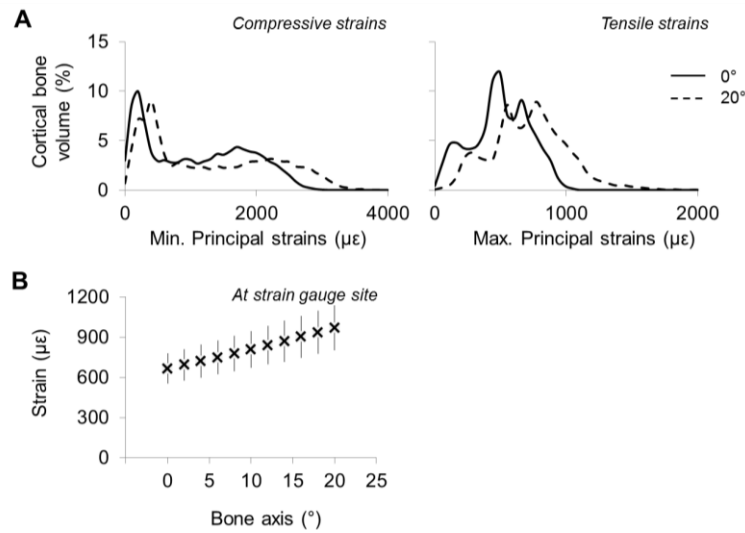


**Fig. 8** (A) Distribution of minimum (compressive) and maximum (tensile) principal strains at the cortical mid-diaphysis of mouse tibia while modifying the bone axis with respect to load trajectory from 0° to 20° (B) Average and standard deviation of longitudinal strains at strain gauge site in different tibia alignment conditions
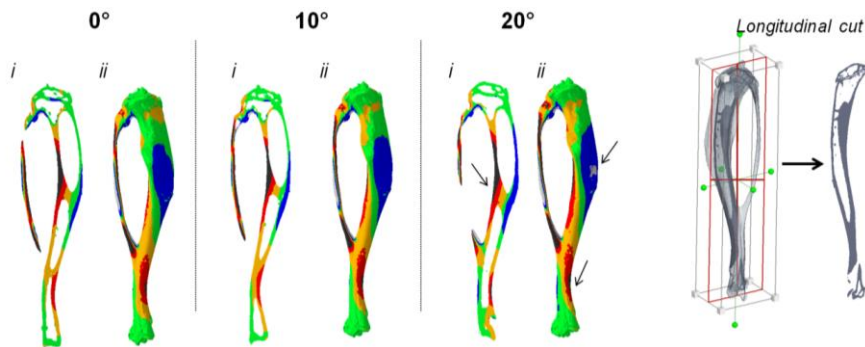


**Fig. 9** Distribution of absolute maximum principal strains within the mouse tibia (i: longitudinal cross-section of tibia, ii: anteromedial perspective to tibia) while modifying the bone axis with respect to load trajectory from 0° (left) to 10° (middle) and to 20° (right). Arrows point to regions with large differences between models

## 4. DISCUSSION

So far, the direct link between *in vivo* bone loading, tissue adaptation and local mechanical strain stimulus remains unclear. A major reason is the lack of knowledge on the local mechanical strain and how it depends upon the local *in vivo* bone loading. Finite element modeling is a powerful tool to characterize the local mechanical straining of bone. *In vivo* mouse tibia loading experiment is a popular method to investigate the mechano-biological tissue adaptation relationships. Such controlled animal loading model surpasses the complicated burden of accurately identifying the strain environment during normal physiological daily activities (e.g. walking, running). However, to link local biological reactions to the local mechanical stimuli requires exact modeling of the loading environment in the bones. Finite element models to characterize the mechanical environment during tibia loading are subjected to uncertainties regarding the boundary conditions and bone positioning in the experimental set-up. In this study, we investigated the influence of variation in boundary conditions and bone alignment in the loading machine on the predicted strains at the tibia mid-diaphysis and strain gauge position. Bone alignment, joint contact surfaces and displacement/rotational constraints at the boundaries were investigated for their potential influence on the predicted strains.

We have observed that alterations in joint contact surfaces where the boundary conditions are applied have a small effect on the general strain state within the bone diaphyseal region. However, large variations are observed at closer proximity to the boundary, i.e. proximal and distal metaphyseal regions. Previous studies have used different boundary conditions to characterize the mechanical environment in the *in vivo* tibial compression mouse model [3, 4, 7, 9-12]. Patel et al. cropped proximal and distal parts of the bone to apply the boundary conditions to the FEM [10] (similar to [12]). Other reports have used a 3D reconstructed bone volume and selected the entire articulation surfaces at the knee and ankle joints of murine tibia to apply the boundary conditions [11] (and similarly [4]). Yang et al. have assigned the boundary conditions on two elliptical surfaces at the knee side (similar to our A2-B2 mode) [9]. Our results are comparable in terms of general strains state within the diaphyseal bone regions to previous reports [4, 9-11]. However, Patel et al. have reported up to 3000 $\mu\varepsilon$ compressive strain at the proximal metaphyseal region [10], which is 2000 $\mu\varepsilon$ higher than our findings at the same region. These differences can be explained by the fact that in their model cutting the bone boundaries might have eliminated the propagation of deformation into the cancellous bone resulting in the shielding of strain by the outer cortical bone. However, our results at the metaphyseal regions are in close agreement with previous reports where either the entire knee articulation surface [11] or part of this surface [9] is used for application of the boundary conditions.

Assigning displacement constraints might seem trivial. The general consensus is to fix displacement in all degrees of freedom at one joint and insert the loading conditions in the other joint. In addition, a displacement constraint in the direction perpendicular to the load axis is introduced allowing only axial movement to the corresponding joint [3, 4, 9-12]. However, it is likely that the bone moves within the cup and platen while the animal is within the loading machine, since there are no restraints to avoid small movements. Yang et al. report the highest sensitivity index in their FE model of the mouse tibia compression loading due to the choice of proximal displacement constraints [9]. A large influence is shown by their FE models between allowing and completely restraining the

displacement of the knee side in the transverse plane perpendicular to the load. Our results are in agreement with this report [9] by showing large differences between predicted strains in these two constraint states (constraint 1 and constraint 3). These results show that proximal constraints largely affect the induced strain magnitudes within the mouse tibia (Fig. 6-7). In addition, the predicted strains at the gauge site are largely affected by this variation (up to 150%).

Another parameter when modeling the *in vivo* loading experiment is the bone alignment in the experimental set-up. Due to the nature of bone being encapsulated in the soft tissue and muscles, and also being in contact with other neighboring bones, accurate estimation of bone alignment within every single experimental set-up is difficult. Positions of peak strains have been shown not to be affected by inclusion of misalignment in the rodent tail model [16]. In the mouse axial compression loading experiment, it has been shown that the initial misalignment of the tibia is not affecting the induced strains since it is automatically adjusted during the loading experiment to the axial loading position, likely due to the geometry of the fixtures holding the knee and the foot in place [17]. It remains unclear how the knee and foot are situated within the holders after this initial automatic adjustment. It is shown that in order to match the experimental prediction of the neutral axis in the mouse tibia model, inclusion of a lateral force in the FE model is inevitable [10]. This finding suggests that the mouse tibia in the axial compression loading experiment exhibits a small misalignment. We identified the effect of varied bone misalignments on the induced strains. The general strain state induced at the tibia was not affected by introducing a tilt angle; however, since changing the load direction leads to changes in the bending moment in mouse tibia, strain induced in mouse tibia varied with bone orientation. In the anticipated range of misalignments; from 0° to 20° (higher tilt angles would be visually obvious or intolerable in the machine fixtures) up to +300 με (40%) difference is introduced in the predicted strains at the strain gauge site.

Bone material property plays a key role in the determination of the strain environment within bone tissue. In the current study, we have implemented 20 GPa isotropic and homogeneous elastic moduli in order to investigate the effect of various boundary conditions on the predicted strains within the bone. However, it is worth noting that neither of our different configurations of boundary conditions did match the *in vivo* measured experimental strains at the gauge position. Indeed up to 70% difference between the predicted and the measured strains at the gauge position was determined indicating a possible influential role of the material elastic properties. In a recent report, our group has shown how heterogeneous material properties affect the strain magnitudes within the mouse tibia, especially at the sites closer to the proximal and distal regions [14].

Characterizing the induced strains within the mouse tibia is a crucial step that helps identifying the mechanical regulation of tibial structural adaptation to external loading regimes. Although much effort has been made to characterize the strain environment induced within the mouse tibia in the *in vivo* compression loading experiment [2-5, 9-12, 17], consistent results are not yet achieved. Unclear modeling parameters such as bone alignment, joint contact surfaces and movement/displacement constraints at the proximal and distal bone regions might explain this inconsistency. In this study, we have shown that although the general strain state within the mouse tibia under compressive loading is not affected by these uncertain parameters, the strain magnitudes at various tibial regions are highly influenced by certain modeling assumptions such as displacement constraints. We

have found that the assignment of displacement constraints has a strong influence on the predicted strains at the mid-shaft region in the mouse tibia. In addition, our results show that the joint contact surfaces mainly influence the strain magnitude and distribution at the proximal metaphyseal region without affecting the diaphyseal region of the tibia. Our results clearly demonstrate the importance of appropriate selection of model parameters when developing a finite element models to predict strains induced within the bone.

## References

1. Schulte F.A., Ruffoni D., Lambers F.M., Christen D., Webster D.J., Kuhn G., Muller R., 2013, *Local mechanical stimuli regulate bone formation and resorption in mice at the tissue level*, PLOS One 8(4): e62172. doi: 10.1371/journal.pone.0062172

2. Lynch M.E., Main R.P., Xu Q., Walsh D.J., Schaffler M.B., Wright T.M., van der Meulen M.C., 2010, *Cancellous bone adaptation to tibial compression is not sex dependent in growing mice*, Journal of Applied Physiology 109(3), pp. 685-91.

3. Willie B.M., Birkhold A.I., Razi H., Thiele T., Aido M., Kruck B., Schill A., Checa S., Main R.P., Duda G.N., 2013, *Diminished response to in vivo mechanical loading in trabecular and not cortical bone in adulthood of female C57Bl/6 mice coincides with a reduction in deformation to load*, Bone 55(2), pp. 335-46.

4. Moustafa A., Sugiyama T., Prasad J., Zaman G., Gross T.S., Lanyon L.E., Price J.S., 2012, *Mechanical loading-related changes in osteocyte sclerostin expression in mice are more closely associated with the subsequent osteogenic response than the peak strains engendered*, Osteoporosis International 23(4), pp.1225-34.

5. Lynch M.E., Brooks D., Mohanan S., Lee M.J., Polamraju P., Dent K., Bonassar L.J., van der Meulen M.C., Fischbach C., 2013, *In vivo tibial compression decreases osteolysis and tumor formation in a human metastatic breast cancer model*, Journal of Bone and Mineral Research 28(11), pp.2357-67.

6. Weatherholt A.M., Fuchs R.K., Warden S.J., 2013, *Cortical and trabecular bone adaptation to incremental load magnitudes using the mouse tibial axial compression loading model*, Bone 52(1), pp. 372-9.

7. Birkhold A.I., Razi H., Duda G.N., Weinkamer R., Checa S., Willie B.M., 2014, *The influence of age on adaptive bone formation and bone resorption*, Biomaterials 35(34), pp. 9290-301.

8. Birkhold A.I., Razi H., Duda G.N., Weinkamer R., Checa S., Willie B.M., 2014, *Mineralizing surface is the main target of mechanical stimulation independent of age: 3D dynamic in vivo morphometry*, Bone 66(), pp. 15-25.

9. Yang H., Butz K.D., Duffy D., Niebur G.L., Nauman E.A., Main R.P.., 2014, *Characterization of cancellous and cortical bone strain in the in vivo mouse tibial loading model using microCT-based finite element analysis,* Bone, 66, pp. 131-9.

10. Patel T.K., Brodt M.D., Silva M.J., 2014, *Experimental and finite element analysis of strains induced by axial tibial compression in young-adult and old female C57Bl/6 mice*, Journal of Biomechanics 47(2), pp. 451-7.

11. Stadelmann V.A., Hocke J., Verhelle J., Forster V., Merlini F., Terrier A., Pioletti D.P., 2009, *3D strain map of axially loaded mouse tibia: a numerical analysis validated by experimental measurements*, Computer Methods in Biomechanics and Biomedical Engineering 12(1), pp. 95-100.

12. Connelly J.T., Fritton J. C., van der Meulen, M. C., 2003, *Simulation of in vivo loading in the tibia of the C57BL/6 mouse*, 49th Annual Meeting of the Orthopaedic Research Society, Poster #0409, New Orleans, LA.

13. Bouxsein M.L., Boyd S.K., Christiansen B.A., Guldberg R.E., Jepsen K.J., Muller R., 2010, *Guidelines for assessment of bone microstructure in rodents using micro-computed tomography*, Journal of Bone and Mineral Research 25(7), pp. 1468-86.

14.  Razi H., Birkhold A.I., Zaslansky P., Weinkamer R., Duda G.N., Willie B.M., Checa S., 2014, *Skeletal maturity leads to a reduction in the strain magnitudes induced within the bone: a murine tibia study*, Acta Biomaterialia, available online: doi:10.1016/j.actbio.2014.11.021
15.  Zilske M., Lemecker H., Zachow S., 2008,  *Adaptive Remeshing of Non-Manifold Surfaces*. Proceedings of Eurographics 2008, Crete, Greece, pp. 207-211.
16.  Goff M.G., Chang K.L., Litts E.N., Hernandez C.J., 2014, *The effects of misalignment during in vivo loading of bone: Techniques to detect the proximity of objects in three-dimensional models*, Journal of Biomechanics 47(12), pp. 3156-61.
17.  Carriero A., Abela L., Pitsillides A.A., Shefelbine S.J., 2014, *Ex vivo determination of bone tissue strains for an in vivo mouse tibial loading model*, Journal of Biomechanics 47(10), pp. 2490-7.

# MODEL KONAČNIH ELEMENATA ZA OPTEREĆENJE SABIJANJEM TIBIJE MIŠA *IN VIVO*: UTICAJ GRANIČNIH USLOVA

Iako je poznata sposobnost kosti da se prilagodi mehaničkim izazovima, odnos između lokalnog mehaničkog stimulansa i reakcije prilagodljivog tkiva za sada izgleda nejasan. Glavni izazov izgleda da predstavlja pravilna karakterizacija lokalnog mehaničkog stimulansa kostiju (naprezanja). Metod konačnih elemenata je moćan alat za karakterizaciju ovih mehaničkih stimulansa ne samo na površini kostiju već i u tkivu. Međutim, razvijanje predvidljivog modela konačnih elemenata za naprezanje biološkog tkiva (na primer, naprezanja poput fiziološkog) nailazi na aspekte koji su neizbežno nejasni ili magloviti što može znatno uticati na predviđene rezultate. Naš cilj je bio da ispitamo uticaj varijacija u naleganju kostiju, dodirnih površina zgloba i ograničenja izmeštanja na predviđena naprezanja u eksperimentu sa opterećenjem sabijanjem tibije kod miša in vivo. Utvrdili smo da  opšte stanje naprezanja u tibiji miša pod opterećenjem sabijanjem nije bilo pod uticajem ovih neizvesnih faktora. Međutim, veličine naprezanja na različitim područjima tibije bili su pod velikim uticajem specifičnih pretpostavki modeliranja. Ograničenja izmeštanja radi kontrole dodirnih površina zgloba, po svemu sudeći, bili su najznačajniji faktor od uticaja na predviđena naprezanja u tibiji miša. Naprezanja su mogla da variraju do 150% izmenom kinematskih ograničenja. U manjoj meri, loše naleganje kostiju (od 0 do 20°) takođe je ishodovalo promenom naprezanja (+300 $\mu\varepsilon$ = 40%). Izbor dodirnih površina zgloba mogao je da dovede čak do variranja od 6%. Naši rezultati pokazuju značaj specifičnih graničnih uslova u eksperimentu sa opterećenjem tibije miša in vivo radi predviđanja vrednosti lokalnih mehaničkih naprezanja pomoću modeliranja konačnim elementima.

Ključne reči: *model konačnih elemenata, opterećenje tibije miša, prilagođavanje kostiju, mehanika kostiju*